

Laser-induced forces on atoms during ultrafast demagnetization

G. P. Zhang*

Department of Physics, Indiana State University, Terre Haute, Indiana 47809, USA

Y. H. Bai

*Office of Information Technology, Indiana State
University, Terre Haute, Indiana 47809, USA*

(Dated: September 7, 2022)

Abstract

Laser-induced femtosecond demagnetization has attracted a broad attention as a possible candidate for information storage technology. However, whether or not lattice vibration directly participates in demagnetization has been highly controversial over a decade. A recent electron diffraction experiment attributed the demagnetization to the polarized phonon effect, but a similar x-ray diffraction experiment attributed it to the Einstein-de Haas effect. Common to both experiments is that neither the angular momentum of the lattice nor the rotation of the sample was directly probed. Here, we report our first first-principles calculation of forces on atoms induced by an ultrafast laser during ultrafast demagnetization. We employ two complementary methods: (i) the frozen lattice with electronic excitation and (ii) frozen excitation but moving the lattice. We find that the forces on atoms start at -50 fs and peak around 30 fs. The magnitude of the force is far smaller than the empirical estimates. Within the limit of our theory, our results suggest that the polarized phonon effect and the Einstein-de Haas effect are unlikely to be the main course of demagnetization. We expect that our finding has a profound impact on the future direction of laser-induced dynamics in magnetic and quantum materials.

PACS numbers:

Keywords:

I. INTRODUCTION

In 1996, Beaurepaire and his coworkers [1] reported that a 60-fs laser pulse can quench the magnetization of a nickel thin film more than 40% within 1 ps. This pioneering discovery has forever changed the landscape of spin manipulation, where a laser field, instead of a magnetic field, is employed. The accelerated demagnetization, found in many magnetic materials [2–8], has attracted enormous attentions across several decades around the world [9, 10], for a historical account of the discovery of femtomagnetism, see a recent book [11]. This unprecedented ultrashort time scale involves a large group of interactions among electrons, spins, orbitals and phonons, either directly or indirectly, which significantly complicates femtomagnetism [9]. The first theory [12] emphasized a crucial interplay between the laser field and the spin-orbit coupling, so the spin symmetry can be broken and the spin moment can be changed. Subsequent mechanisms invoke the phonon-based Elliot-Yafet mechanism [13, 14] with the spin flipping through the spin-orbit coupling [12], spin transport with majority spin moving out of the excited region [15], bands mirroring effect [16] with the spin majority and minority switching their roles, spin-wave excitation [17] across many lattice sites to reduce the spin moment for the entire sample, spin disordering [18] within a big cell, ultrafast electron correlations and memory effects [19] through the dynamic exchange kernel, optical inter-site spin transfer [20], and electron-phonon scattering [21]. The fact that so many mechanisms were proposed demonstrates the complexity of femtomagnetism. To this end, no single mechanism can explain all the experimental observations; and probably it may never be possible, given the fact that diverse materials show different dynamics. For instance, Fe and Gd have quite different demagnetization processes [7].

Another line of thought is formulated around the spin angular momentum transfer [22–24], without considering the fact that the total angular momentum operator is not a conserved quantity in solids [25]. Once this total angular momentum conservation is assumed, then it is easy to see that if the spin angular momentum of the electron system cannot transfer to the orbital angular momentum of the electron [26], it must go to the lattice [27]. Although this mechanism cannot exclude other mechanisms such as spin quenching due to the spin misalignment, it underlines two recent experimental investigations [28, 29]. However, to this end, no experiment ever *directly* measured the rotation of samples or the lattice angular momentum as one should if this is due to the Einstein-de Haas effect. Dornes *et al.* [28]

employed the time-resolved X-ray diffraction as the probe and 40-fs laser pulse of 800 nm as the pump and measured the transverse strain wave, from which they inferred through modeling that 80% spin angular momentum in the Fe film went to the lattice within 200 fs. Tauchert *et al.* [29] carried out the electron diffraction experiment and found the Bragg spot position from their Ni film did not change with time within their experimental uncertainty, so there was no transient strain or lattice expansion, contradicting the finding by Dornes *et al.* [28]. It is difficult to argue that the different conclusions reached from these two experiments are due to the technique difference, as electron diffraction should induce more strain than X-ray diffraction. Instead, Tauchert *et al.* [29] found an anisotropic diffraction pattern that follows the initial magnetization of their sample, which they attributed to the polarized phonon involvement, but phonons are rarely magnetically active [30] and the long-lasting associated orbital moment of the electron observed in He atoms [31] cast doubts on this interpretation. The key to resolve these difficult issues is to find the force on the atoms. If the force is centripetal, then the postulate of the polarized phonon is valid.

Theory can help in this regard by tracing back to the initial stage of laser excitation, where electrons are newly excited out of the Fermi sea and the force starts to appear on atoms. In this paper, we develop a scheme that combines the ground state density functional theory and the time-dependent Liouville formalism in a supercell. This allows us to compute the force on the atoms during the laser-induced ultrafast demagnetization. We employ one free-standing Ni(001) monolayer as our first example. We find that the force on the Ni atom starts around -50 fs, followed by a rapid oscillation due to the strong charge fluctuation. The force ceases to change once the electronic excitation configuration is formed. Quantitatively, we find that under moderately strong laser pulse excitation, the amplitude of force is 0.01 mRy/a.u., which is far below the estimate based on the Tauchert's parameter [29]. Although the force does change directions during the laser excitation, we do not detect evidence of the centripetal force as required by the polarized phonon. Our results in fcc Ni further show that the directions of forces on all four Ni atoms do not change. Therefore, our present theoretical results, within the limit of our current theory, do not support the picture of the polarized phonons. This finding is expected to motivate further experimental and theoretical investigations in the future.

The rest of the paper is arranged as follows. In Sec. II, we present our theoretical algorithm, which combines the ground state calculation and the time-dependent Liouville

equation. Section III is devoted to (i) the results in the Ni(001) monolayer, (ii) the effect of core states and the spin polarization on the force, and (iii) the results in fcc Ni. We conclude this paper in Sec. IV.

II. THEORETICAL FORMALISM

Laser-driven ultrafast demagnetization starts with the electronic excitation which tip the balance of force on atoms. Figure 1 schematically shows a typical laser excitation. A laser pulse excites the electron first and through the electron-lattice interaction, atoms experience a net force. So the key to resolve the above controversy is to directly compute the forces on atoms under laser excitation. If the force is centripetal, then the atoms will undergo a circular motion. However, such a calculation is difficult, if not impossible, since a solid has highly coupled interactions among electron, spin and lattice dynamics over several hundred fs in a supercell. This is part of the reason why so far there has been no theory attempt to compute forces. We find a method that integrates two complementary algorithms into a well-defined formalism.

The top left of Fig. 1 shows that our density-functional theoretical calculation starts with the ground state calculation, by solving the Kohn-Sham equation self-consistently [32],

$$\left[-\frac{\hbar^2 \nabla^2}{2m_e} + v_{eff}(\mathbf{r}) \right] \psi_{i\mathbf{k}}(\mathbf{r}) = E_{i\mathbf{k}} \psi_{i\mathbf{k}}(\mathbf{r}), \quad (1)$$

where $\psi_{i\mathbf{k}}(\mathbf{r})$ and $E_{i\mathbf{k}}$ are, respectively, the eigenstate and eigenenergy of band i and \mathbf{k} point. v_{eff} is determined by

$$v_{eff}(\mathbf{r}) = v(\mathbf{r}) + \int \frac{n(\mathbf{r}')}{|\mathbf{r} - \mathbf{r}'|} d\mathbf{r}' + v_{xc}(\mathbf{r}), \quad (2)$$

where $v_{xc}(\mathbf{r})$ is the exchange-correlation potential, $v_{xc}(\mathbf{r}) = \delta E_{xc}[n]/\delta n(\mathbf{r})$. We employ the Wien2k code, which uses the full-potential augmented planewave basis. The spin-orbit coupling is included through the second variational principle [33]. We use the generalized gradient approximation for the exchange-correlation energy functional.

The forces on atom α contain several contributions. The Hellmann-Feynman (HF) force in the atomic units is [34]

$$\mathbf{F}^\alpha = z_\alpha \frac{d}{d\tau_\alpha} \left(- \sum'_\beta \sum_{\mathbf{R}} \frac{z_\beta}{|\tau_\alpha - \tau_\beta + \mathbf{R}|} + \int \frac{n(\mathbf{r})}{|\tau_\alpha - \mathbf{r}|} d\mathbf{r} \right), \quad (3)$$

where z_α is the atomic number, τ_α is its position in a unit cell, and \mathbf{R} is the lattice vector. The prime over the summation excludes the same atom. This force is common among all the methods. In LAPW, the states are separated into core states, semicore state, and valence states. The core correction to the HF force is

$$\mathbf{F}_{\text{core}}^\alpha = - \int \rho_c^\alpha(\mathbf{r}) \nabla v_{\text{eff}}(\mathbf{r}) d\mathbf{r}, \quad (4)$$

where $\rho_c^\alpha(\mathbf{r})$ is the core charge density at atom α . The treatment of valence states is more complicated due to the incomplete basis-function set (IBS) that is associated with the LAPW basis function,

$$\mathbf{F}_{\text{IBS}} = - \sum_i \rho_i (\langle \psi'_i | (H - \epsilon_i) | \psi_i \rangle + \langle \psi_i | (H - \epsilon_i) | \psi'_i \rangle + \mathbf{D}_i), \quad (5)$$

where ρ_i is the occupation number of valence state i , ϵ_i is the eigenvalue, H is the Kohn-Sham Hamiltonian, ψ_i is the eigenfunction, and ψ'_i denotes its derivative with respect to the atomic position τ_α . \mathbf{D}_i is the kinetic energy contribution due to the change in both the MT sphere and the interstitial regions [34, 35]. The total force is the sum of the HF force, the core and IBS corrections. Wien2k has a limitation that its force has no contribution from the spin-orbit coupling (SOC) even if we include SOC. Since SOC in general is a weak contributor energetically, we do not expect that missing force from SOC has a qualitative effect on our force.

Upon laser excitation, electrons are first excited out of the Fermi sea. We employ the time-dependent Liouville equation [32, 36]

$$i\hbar \frac{\partial \rho}{\partial t} = [H_0 + H_I, \rho], \quad (6)$$

where H_0 is the unperturbed system Hamiltonian and H_I is the interaction between the laser field and the system [36], $H_I = -\mathbf{p} \cdot \mathbf{A}(t)/m_e$. The vector potential is $\mathbf{A}(t) = A_0 \exp(-t^2/\tau^2)(\cos \omega t \hat{x} + \sin \omega t \hat{y})$, where A_0 is the amplitude, τ is the laser pulse duration, t is the time, \hat{x} and \hat{y} are the unit vectors of the x and y axes, respectively, and the laser polarization is within the xy plane. We note in passing that the fluence of laser field is computed from [11]

$$\mathcal{F}(\omega, \tau) = \sqrt{\frac{\pi}{2}} n(\omega) c \epsilon_0 A_0^2 \omega^2 \tau, \quad (7)$$

where c is the speed of light, $n(\omega)$ is the index of refraction, and τ is the pulse duration.

We only propagate our time step from t to $t + \Delta t$. The right figure of Fig. 1 outlines the key steps of our implementation. The excited state density ρ is used to construct the excited state density and is fed back into Eq. 1 for an excited state self-consistent calculation [32]. The shaded box highlights this self-consistency. The converged density is looped back into the Liouville equation (Eq. 6) to start a new time step.

III. RESULTS AND DISCUSSIONS

Traditional force calculations in solids often adopt a single Γ point [37], which is apparently unsuitable for metals. We propose a different formalism to tackle this issue. We freeze the lattice in the same fashion as the frozen phonon calculation, and then directly compute the forces on the atoms during laser excitation. Regardless of whether angular momentum transfer or electron-lattice coupling is central to demagnetization, the lattice must experience a force in order to vibrate.

A. Nickel(001) monolayer

We take a free-standing nickel(001) monolayer as an example. Since its primitive cell has no net force on atoms, we adopt a $2 \times 2 \times 1$ supercell, with two distinctive atoms Ni_1 and Ni_2 at $(0,0,0)$ and $(1/2,1/2,0)$, respectively. We insert a vacuum layer of thickness 33 bohr along the c axis to eliminate the interaction between each layer. We choose a k mesh of $20 \times 20 \times 1$ in the crystal momentum space. The product of the muffin-tin radius and the planewave cutoff $R_{\text{MT}}K_{\text{max}}$ is 7.

Forces in the ground state – We displace the Ni_1 atom along the x axis by a small amount δx_1 from -5% to +5%, in the unit of the lattice constant a . Figure 2(a) displays the total energy change ΔE as a function of δx_1 , where a typical parabola is observed. Here the energy is referenced to the minimum energy. Forces on atoms are shown in Fig. 2(b). Since we move Ni_1 along the x axis, the main force is along the x axis, while the forces along the y are tiny (see the lines close to 0). The empty (filled) circles denote the force F_{1x} (F_{2x}) on Ni_1 (Ni_2). F_{1x} and F_{2x} have an opposite slope as expected. The force slope gives an estimate of the angular frequency of 10.76 THz for Ni, representing an upper bound phonon frequency in the electronic ground state.

Forces in the excited state – We employ a circularly polarized pulse of $\tau = 60$ fs and the photon energy is $\hbar\omega = 1.6$ eV. We choose a vector field amplitude $A_0 = 0.03$ Vfs/Å, which corresponds to a fluence of 10.61 mJ/cm², very typical experimentally [1, 28, 29, 38]. The full-width at half-maximum of the pulse is about 100 fs. Figure 2(c) is the energy change as a function of time. We see the system absorbs the energy quickly upon laser excitation; the entire process starts at -100 fs and ends around 100 fs. Our interest is in the force. Figure 2(d) shows the force on Ni₁, and the force on Ni₂ is similar and not shown. F_{1x} gains an appreciable value around -50 fs, and then it starts a rapid oscillation. We verify that these rapid oscillations are from the charge fluctuation during the time propagation of density. The spikes seen in the force in the self-consistent step appear from one time step to next. Our time step is 1/32 the laser period. We run four separate calculations under different conditions, with or without the core states and with or without spin-polarization rescaling [32], to verify that while details of these rapid oscillations may differ from one to another, the general pattern is highly reproducible. Naturally, atoms cannot respond to these rapid oscillations, and the force after these rapid oscillations is important. If the polarized phonon concept [29] is valid, we are supposed to see the force direction change periodically. This direction change is barely observed around 42 fs, where F_{1y} transitions from a positive force to a negative one, while F_{1x} does the opposite. However, after 50 fs, both force components settle down, and there is no evidence of centripetal force from our data.

Tauchert *et al.* [29] carried out ultrafast electron diffraction to detect the motion of Ni atoms in a nickel single crystal layer after optical excitation. They found no change in the Bragg spot broadening and no change in lattice displacement, but the intensity ratio between (200) and (020) planes depends on the direction of the applied magnetic field. They attributed this difference to the polarized phonon. They assumed that the 50% spin angular momentum loss is converted to the circular motion of the Ni atom,

$$\Delta L = M_{\text{Ni}}\omega R^2 = 0.16\hbar, \quad (8)$$

where ω is angular frequency, M_{Ni} is the atomic mass of Ni, and R is the radius of the circular motion of 0.019 Å [29]. Because the centripetal force on the atom is

$$F = M_{\text{Ni}}\omega^2 R, \quad (9)$$

we combine Eqs. 8 and 9 to rewrite the force as

$$F = \omega\Delta L/R. \quad (10)$$

This expression has a nice feature where the force is independent of mass, thus eliminating the material difference between Dornes [28] and Tauchert [29]. The only remaining quantity is ω . Unfortunately, there is no information on ω . Due to the translation symmetry in solids, a single normal mode never undergoes a circular motion, qualitatively different from molecular crystals [39]. Tauchert *et al.* [29] interpreted the highest phonon frequency of 8 THz found in the nickel phonon spectrum as ω , which in general is incorrect or questionable. But using it, we can estimate the force from their data to be 10.84 mRy/bohr per atom, a value that we can compare with.

Figure 2(d) presents a different picture. Our force is only 0.01 mRy/bohr, three orders of magnitude less than theirs. 10.84 mRy/bohr is also too large for the ground state. If one used the same slope of the force as Fig. 2(b), 10.84 mRy/bohr would translate δx_1 to be 10%, or 0.3 Å, which is really too large for nuclear vibrations. In C₆₀, we find [39] the lattice displacement around 0.05 Å. Up to now, our lattice is frozen. What if we release it in the electronic excited state? We choose an electronic excited configuration around 566 fs, and then displace Ni₁ along the x axis, just as we did for the ground state in Fig. 2(b). Figure 2(e) shows the total energy change as a function of δx_1 . We find that in the electronic excited state, the parabola is steeper. For the same δx_1 , $\Delta E_{ex} = 7 \times 10^{-5}$ Ry, larger than $\Delta E_{gs} = 3.2 \times 10^{-5}$ Ry. The force changes are shown in Fig. 2(f). It is clear that the force change is more complex and no longer has a linear relation with δx_1 . If δx_1 is smaller than $\pm 1\%$, the dependence is similar to the ground state (see Fig. 2(b)). But as soon as δx_1 is larger than $\pm 2\%$, F_{1x} decreases with δx_1 . F_{2x} shows an opposite trend. In the ground state, F_{1y} and F_{2y} are very small, but now in the excited state, they become appreciable. If we compare the force magnitudes between Figs. 2(d) and 2(f), we see that the force reaches 1 mRy/bohr. This shows that our excited state force in Fig. 2(d) is a lower limit. But the force at the maximum is still 10 times smaller than Tauchert's force.

B. Effect of core states and spin polarization scaling on the force

Since there has been no prior study on the laser-induced force on atoms during demagnetization, we carry out four complementary tests to iron out some of possible scenarios that Wien2k could provide.

We first examine the effect of core states on our force. The Ni-L edge has eight core states

($3s^23p^6$) for each Ni atom, which locate 65 eV below the Fermi level. There are 10 valence electrons ($3d^84s^2$ or $3d^94s^1$). A single excitation from 1.6-eV photons rarely affects the core states, but multiple excitations do. Since core states have a larger contribution to the force, their effect is of interest. For these reasons, a direct test is necessary. Our time-dependent Liouville equation can conveniently select a group of states with a particular window. Figure 3(a) includes states from 5 ($3p^6$) to 100 (20 eV from the Fermi level), which covers the core states, all the valence states and 66 conduction states. This is the same data for our Fig. 2(d). By contrast, Fig. 3(b) includes all the valence states but does not include core states. All the rest of the parameters, including the laser parameters, are the same. We see that their general trend remains similar, but there is a clear difference: Figure 3(a) has a negative F_{1x} , but Figure 3(b) has a positive F_{1x} . The direction of F_{1y} is also exchanged. This shows that the core states do contribute. We also understand why. Although the core states do not directly participate in the optical excitation, the force from the core state contains a correction term (Eq. 4) due to the effective potential v_{eff} . And this v_{eff} depends on the electron density $\rho(\mathbf{r})$. So during the laser excitation, once ρ changes, the force due to the core state changes.

Next, we investigate whether the spin-polarization scaling factor [32] affects the forces. This scaling is used in the spin-polarized potential. For α electron, the potential is

$$V_\alpha(\mathbf{r}, t) = \frac{1}{2} [(1 + \xi(t))V_\alpha(\mathbf{r}) + (1 - \xi(t))V_\beta(\mathbf{r})] \quad (11)$$

where $\xi(t) = M(t)/M_0$ is computed from the spin moment $M(t)$. A similar equation for β electron. If we set $\xi(t) = 1$, this means that we do not have scaling. If $\xi(t) < 1$, the potential is less spin-polarized. Figure 3(c) has neither the core state nor the spin-polarization scaling. We see that those rapid oscillations in the force are suppressed. The force directions are now similar to Fig. 3(a). Finally, we remove the spin-polarization rescaling but keep the core states. Figure 3(d) shows that these rapid oscillations return, and in addition the force is smaller.

In summary, we should mention that our calculations are extremely time consuming, 3-4 months to finish, since for each time step we self-consistently converge the results. During the time when the laser peaks, the convergence criteria are lowered because a large number of conduction states are occupied and the self-consistency becomes difficult. In traditional TDDFT, there is no self-consistency, but in our time-dependent Liouville density functional

theory, we have this extra step. There is another problem that is associated with the Wien2k code. In the excited states, the electrons become very delocalized, so we have to put some electrons as the background charge. This background charge is not used for Figs. 3(a)-(c), but is used for Fig. 3(d). For the moment, we do not find a viable method to overcome this difficulty. A planewave code may help, but it often uses the pseudopotential, where the core states are replaced by a pseudopotential and the effect of the core states on the force on atoms during laser excitation is not possible to investigate.

C. fcc nickel

In order to demonstrate that our conclusion is not limited to the Ni(001) monolayer, we also compute the force on bulk fcc nickel. For the same reason as above, we adopt a simple cubic cell as a supercell for fcc Ni, where we have four atoms per cell and remove all the symmetry operations, except the identity matrix. Figure 4(a) shows the forces on atoms Ni₁ and Ni₂. Since forces on Ni₁ and Ni₂ are similar, we only show that on Ni₁. They do not gain an appreciable value until -70 fs. $F_{1,x}$ points in the x axis, while $F_{1,y}$ points in the $-y$ axis. The magnitude of $F_{1,z}$ is much smaller. At 0 fs when the laser peaks, the force drops to zero. The force peaks around 33 fs, after which it stabilizes around $0.5 \mu\text{Ry}/\text{bohr}$. Figure 4(b) shows the forces on Ni₃ and Ni₄. The general feature is similar. We can estimate how far atoms move, provided the force remains constant. Take the force at $0.5 \mu\text{Ry}/\text{bohr}$ as an example, and we obtain the acceleration a is $0.2114 \times 10^{12} \text{ m/s}^2$. For 1 ps, the atom moves 0.1057 pm, far less than 1.9 pm postulated by Tauchert *et al.* [29]. If we used their time scale of 125 fs (8 THz), the displacement would fall below the thermal disturbance. Importantly, our theory predicts that $F_{1,x}$ and $F_{1,y}$ are 180° out of phase, with the resultant force along the $[1, \bar{1}, 0]$ direction. These forces are unlikely to lead to a circular motion of Ni atoms around the lattice point, because they are not centripetal in any sense. Instead, a regular vibration is expected. This raises a question whether their polarized phonon really exists.

IV. CONCLUSIONS

In contrast to all the prior studies, we have directly computed the laser-induced forces on atoms during ultrafast demagnetization. We find that the force arises around -50 fs before the laser pulse peaks at 0 fs. Due to the strong charge fluctuation, the initial forces are highly oscillatory, and peak around 50 fs, settling down after 100 fs. Although we have observed that the force does change its direction, it does not appear to be centripetal, as would be expected from the polarized phonon picture [29]. Quantitatively, we find the force magnitude is at least one order of magnitude weaker than the early estimate [29]. This conclusion is true for both the Ni(001) monolayer and fcc nickel, within the limit of our current theory. Interestingly, a recent study in He atoms reported the long-lasting orbital moment of the electron [31], not phonon. Could the polarized phonon turn out to be the electron contribution, not the lattice contribution? This likelihood scenario is supported by our theory and also the fact that the experiment employed the electron diffraction, but it can only be resolved with further experimental and theoretical investigations [40, 41].

Acknowledgments

We would like to thank the helpful communication with Dr. Peter Baum (Konstanz, Germany) on their paper [29]. GPZ and YHB were supported by the U.S. Department of Energy under Contract No. DE-FG02-06ER46304. Part of the work was done on Indiana State University's quantum and obsidian clusters. The research used resources of the National Energy Research Scientific Computing Center, which is supported by the Office of Science of the U.S. Department of Energy under Contract No. DE-AC02-05CH11231.

*guo-ping.zhang@outlook.com <https://orcid.org/0000-0002-1792-2701>

-
- [1] E. Beaurepaire, J. C. Merle, A. Daunois, and J.-Y. Bigot, Ultrafast spin dynamics in ferromagnetic nickel, *Phys. Rev. Lett.* **76**, 4250 (1996).
 - [2] J. Hohlfeld, E. Matthias, R. Knorren, and K. H. Bennemann, Nonequilibrium magnetization dynamics of nickel, *Phys. Rev. Lett.* **78**, 4861 (1997).

- [3] M. Aeschlimann, M. Bauer, S. Pawlik, W. Weber, R. Burgermeister, D. Oberli, and H. C. Siegmann, Ultrafast spin-dependent electron dynamics in fcc Co, *Phys. Rev. Lett.* **79**, 5158 (1997).
- [4] G. Ju, A. Vertikov, A. V. Nurmikko, C. Canady, G. Xiao, R. F. C. Farrow, and A. Cebollada, Ultrafast nonequilibrium spin dynamics in a ferromagnetic thin film, *Phys. Rev. B* **57**, R700 (1998).
- [5] T. Roth, A. J. Schellekens, S. Alebrand, O. Schmitt, D. Steil, B. Koopmans, M. Cinchetti, and M. Aeschlimann, Temperature Dependence of Laser-Induced Demagnetization in Ni: A Key for Identifying the Underlying Mechanism, *Phys. Rev. X* **2**, 021006 (2012).
- [6] A. Mann, J. Walowski, M. Münzenberg, S. Matt, M. J. Carey, J. R. Childress, C. Mewes, D. Ebke, V. Drewello, G. Reiss and A. Thomas, Insights into ultrafast demagnetization in pseudogap half-metals, *Phys. Rev. X* **2**, 041008 (2012).
- [7] M. Sultan, U. Atxitia, A. Melnikov, O. Chubykalo-Fesenko, and U. Bovensiepen, Electron- and phonon-mediated ultrafast magnetization dynamics of Gd(0001), *Phys. Rev. B* **85**, 184407 (2012).
- [8] J. Chen et al., *Phys. Rev. Lett.* **122**, 067202 (2019).
- [9] G. P. Zhang, W. Hübner, E. Beaurepaire, and J.-Y. Bigot, Laser-induced ultrafast demagnetization: Femtomagnetism, A new frontier? *Topics Appl. Phys.* **83**, 245 (2002).
- [10] A. Kirilyuk, A. V. Kimel, and Th. Rasing, Ultrafast optical manipulation of magnetic order, *Rev. Mod. Phys.* **82**, 2731 (2010). Erratum: *Rev. Mod. Phys.* **88**, 039904 (2016).
- [11] G. P. Zhang, G. Lefkidis, M. Murakami, W. Hübner, and T. F. George, *Introduction to Ultrafast Phenomena: From Femtosecond Magnetism to High-Harmonic Generation*, CRC Press, Taylor & Francis Group, Boca Raton, Florida (2021).
- [12] G. P. Zhang and W. Hübner, Laser-induced ultrafast demagnetization in ferromagnetic metals, *Phys. Rev. Lett.* **85**, 3025 (2000).
- [13] B. Koopmans, G. Malinowski, F. Dalla Longa, D. Steiauf, M. Fähnle, T. Roth, M. Cinchetti, and M. Aeschlimann, Explaining the paradoxical diversity of ultrafast laser-induced demagnetization, *Nat. Mater.* **9**, 259 (2010).
- [14] A. Born, R. Decker, R. Büchner, R. Haverkamp, K. Rotsalainen, K. Bauer, A. Pietzsch, and A. Föhlisch, Thresholding of the Elliott-Yafet spin-flip scattering in multi-sublattice magnets by the respective exchange energies, *Sci. Rep.* **11**, 1883 (2021).

- [15] M. Battiato, K. Carva, and P. M. Oppeneer, Theory of laser-induced ultrafast superdiffusive spin transport in layered heterostructures, *Phys. Rev. B* **86**, 024404 (2012).
- [16] S. Eich, M. Plötzing, M. Rollinger, S. Emmerich, R. Adam, C. Chen, H. C. Kapteyn, M. M. Murnane, L. Plucinski, D. Steil, B. Stadtmüller, M. Cinchetti, M. Aeschlimann, C. M. Schneider and S. Mathias, Band structure evolution during the ultrafast ferromagnetic-paramagnetic phase transition in cobalt, *Sci. Adv.* **3**, e1602094 (2017).
- [17] G. P. Zhang, M. Murakami, Y. H. Bai, T. F. George, and X. S. Wu, Spin-orbit torque-mediated spin-wave excitation as an alternative paradigm for femtomagnetism, *J. Appl. Phys.* **126**, 103906 (2019).
- [18] Z. H. Chen and L. W. Wang, Role of initial magnetic disorder: A time-dependent ab initio study of ultrafast demagnetization mechanisms, *Sci. Adv.* **8**, eaau8000 (2019).
- [19] S. R. Acharya, V. Turkowski, G. P. Zhang, and T. Rahman, Ultrafast electron correlations and memory effects at work: Femtosecond demagnetization in Ni, *Phys. Rev. Lett.* **125**, 017202 (2020).
- [20] F. Willems, C. von Korff Schmising, C. Strüber, D. Schick, D. W. Engel, J. K. Dewhurst, P. Elliott, S. Sharma, and S. Eisebitt, Optical inter-site spin transfer probed by energy and spin-resolved transient absorption spectroscopy, *Nat. Comm.* **11**, 871 (2020).
- [21] A. Baral, S. Vollmar, and H. C. Schneider, Magnetization dynamics and damping due to electron-phonon scattering in a ferrimagnetic exchange model, *Phys. Rev. B* **90**, 014427 (2014).
- [22] M. Hennecke, I. Radu, R. Abrudan, T. Kachel, K. Holldack, R. Mitzner, A. Tsukamoto, and S. Eisebitt, Angular momentum flow during ultrafast demagnetization of a ferrimagnet, *Phys. Rev. Lett.* **122**, 157202 (2019).
- [23] J. K. Dewhurst, S. Shallcross, P. Elliott, S. Eisebitt, C. v. Korff Schmising, and S. Sharma, Angular momentum redistribution in laser-induced demagnetization, *Phys. Rev. B* **104**, 054438 (2021).
- [24] D. Zahn, F. Jakobs, Y. W. Windsor, H. Seiler, T. Vasileiadis, T. A. Butcher, Y. Qi, D. Engel, U. Atxitia, J. Vorberger, and R. Ernstorfer, Lattice dynamics and ultrafast energy flow between electrons, spins, and phonons in a 3d ferromagnet, *Phys. Rev. Research* **3**, 023032 (2021).
- [25] G. P. Zhang and T. F. George, Total angular momentum conservation in laser-induced femtosecond magnetism, *Phys. Rev. B* **78**, 052407 (2008).

- [26] G. P. Zhang, M. Gu, Y. H. Bai, T. L. Jenkins, and T. F. George, Correlation between spin and orbital dynamics during laser-induced femtosecond demagnetization, *J. Phys. Chem. C* **125**, 14461 (2021).
- [27] C. Stamm, N. Pontius, T. Kachel, M. Wietstruk, and H. A. Dürr, Femtosecond x-ray absorption spectroscopy of spin and orbital angular momentum in photoexcited Ni films during ultrafast demagnetization, *Phys. Rev. B* **81**, 104425 (2010).
- [28] C. Dornes *et al.*, The ultrafast Einstein-de Haas effect, *Nature* **565**, 209 (2019).
- [29] S. R. Tauchert, M. Volkov, D. Ehberger, D. Kazenwadel, M. Evers, H. Lange, A. Donges, A. Book, W. Kreuzpaintner, U. Nowak and P. Baum, Polarized phonons carry angular momentum in ultrafast demagnetization, *Nature* **602**, 73 (2022).
- [30] A. Baydin, F. G. G. Hernandez, M. Rodriguez-Vega, A. K. Okazaki, F. Tay, G. T. Noe II, I. Katayama, J. Takeda, H. Nojiri, P. H. O. Rappl, E. Abramof, G. A. Fiete, and J. Kono, Magnetic Control of Soft Chiral Phonons in PbTe, *Phys. Rev. Lett.* **128**, 075901 (2022).
- [31] J. Wätzel *et al.*, Light-Induced Magnetization at the Nanoscale, *Phys. Rev. Lett.* **128**, 157205 (2022).
- [32] G. P. Zhang, Y. H. Bai, and T. F. George, Ultrafast reduction of exchange splitting in ferromagnetic nickel, *J. Phys.: Condens. Matter* **28**, 236004 (2016).
- [33] P. Blaha, K. Schwarz, G. K. H. Madsen, D. Kvasnicka, and J. Luitz, WIEN2k, An Augmented Plane Wave + Local Orbitals Program for Calculating Crystal Properties (Karlheinz Schwarz, Techn. Universität Wien, Austria, 2001).
- [34] R. Yu, D. Singh, and H. Krakauer, All-electron and pseudopotential force calculations using the linearized-augmented-plane-wave method, *Phys. Rev. B* **8**, 6411 (1991).
- [35] G. K. H. Madsen, P. Blaha, K. Schwarz, E. Sjöstedt, and L. Nordström, Efficient linearization of the augmented plane-wave method, *Phys. Rev. B* **64**, 195134 (2001).
- [36] G. P. Zhang, W. Hübner, G. Lefkidis, Y. Bai, and T. F. George, Paradigm of the time-resolved magneto-optical Kerr effect for femtosecond magnetism, *Nat. Phys.* **5**, 499 (2009).
- [37] W.-H. Liu, J.-W. Luo, S.-S. Li, and L.-W. Wang, The critical role of hot carrier cooling in optically excited structural transitions, *npj Computational Materials* **7**, 117 (2021).
- [38] M. S. Si and G. P. Zhang, Resolving photon-shortage mystery in femtosecond magnetism, *J. Phys.: Condens. Matter* **22**, 076005 (2010).
- [39] G. P. Zhang, Y. H. Bai, and T. F. George, Optically and thermally driven huge lattice orbital

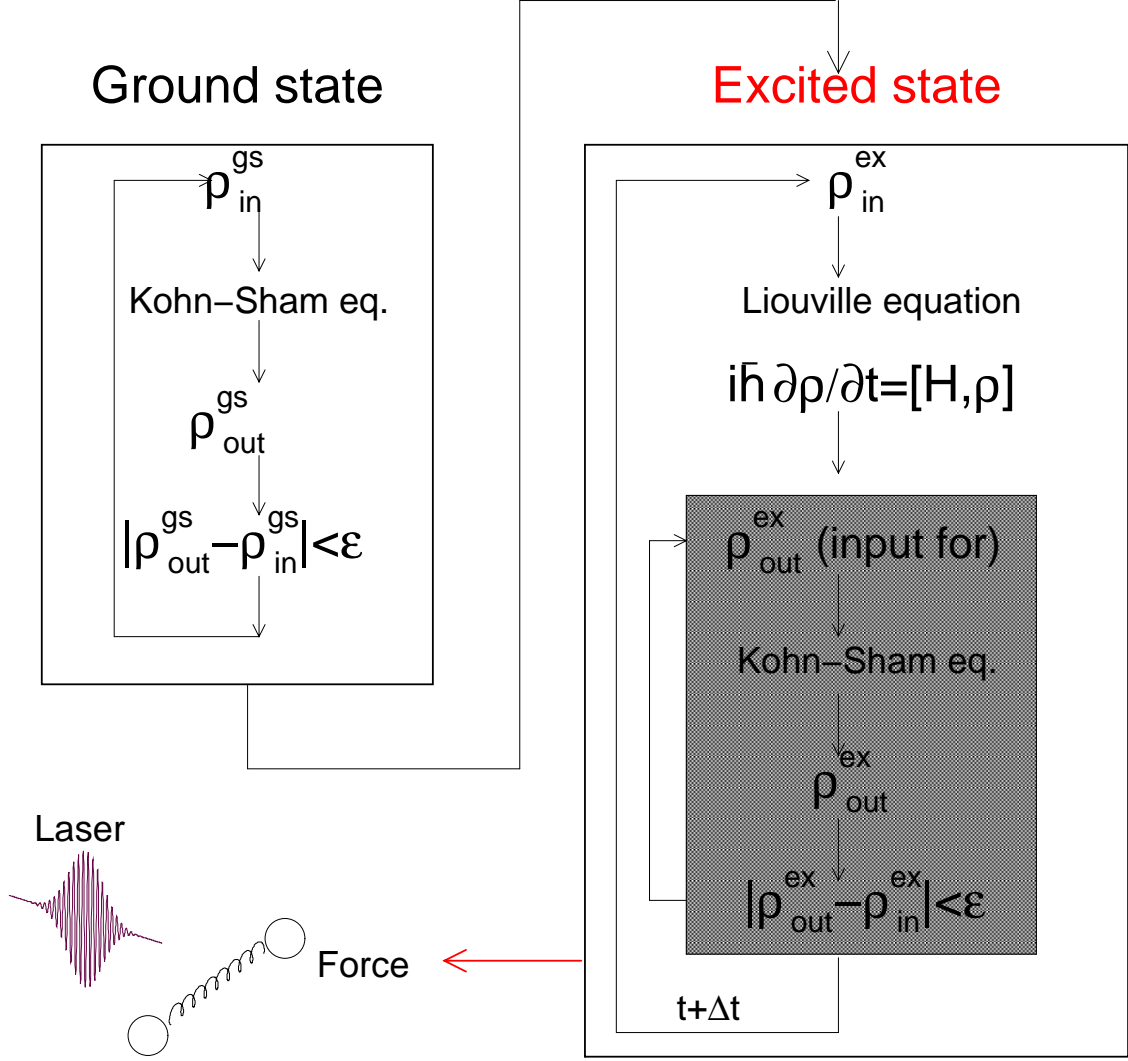


FIG. 1: (Bottom left) Laser-induced force on atoms during the ultrafast demagnetization has an enormous impact on subsequent lattice dynamics. We employ a circularly polarized 60-fs laser pulse σ_{xy} . For a Ni(001) monolayer, a supercell ($2 \times 2 \times 1$) is used. (Top left) Schematic of our theoretical formalism for our ground state calculation. (Right) Time-dependent self-consistent Liouville density functional theory.

and spin angular momenta from spinning fullerenes, Phys. Rev. B **104**, L100302 (2021).

[40] M. Gu, Y. H. Bai, G. P. Zhang, and T. F. George, Spin-phonon dispersion in magnetic materials, J. Phys.: Condens. Matter **34**, 375802 (2022).

[41] S. Mankovsky, S. Polesya, H. Lange, M. Weiß, U. Nowak, and H. Ebert, Angular Momentum Transfer via Relativistic Spin-Lattice Coupling from First Principles, Phys. Rev. Lett. **129**, 067202 (2022).

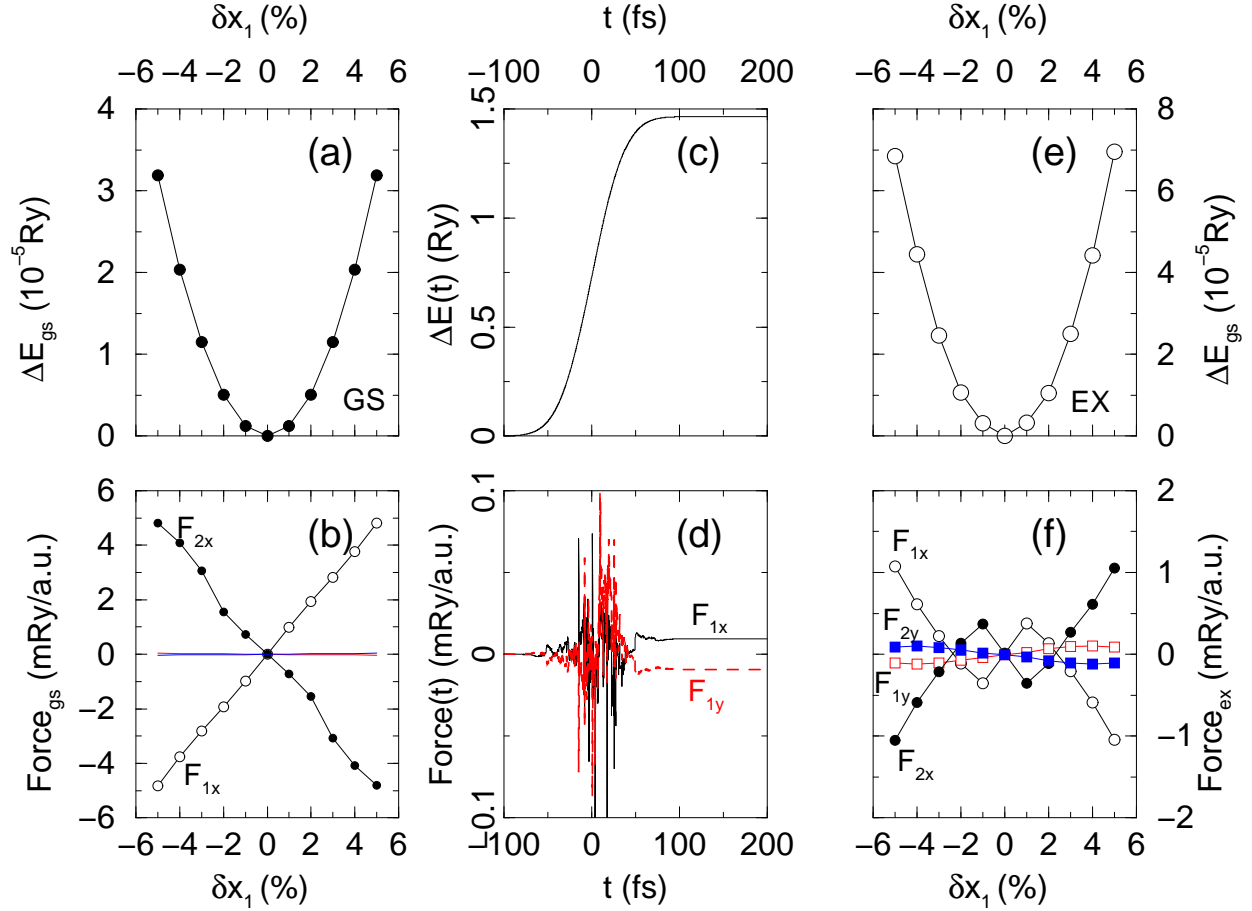


FIG. 2: (a) Total energy change ΔE_{gs} as a function of the Ni_1 position δx_1 in the electronic ground state. δx_1 is in the units of lattice constant a . (b) Force as a function of δx_1 . The open circles denote F_{1x} and the filled circles denote F_{2x} . The y components are small, close to the zero. (c) Under laser excitation, the total energy change $\Delta E(t)$ as a function of time t . The laser pulse has duration of 60 fs, photon energy of 1.6 eV and the vector potential amplitude of 0.03 Vfs/Å. (d) Force on Ni_1 . The solid line represents F_{1x} and the dotted line F_{1y} . Force on Ni_2 is similar, and not shown. (e) In the electronic excited states, the total energy change ΔE_{ex} as a function of δx_1 . (f) In the electronic excited states, the forces on atoms have a different dependence from the ground state counterpart. The unfilled circles denote F_{1x} , and the filled ones F_{2x} . The unfilled and filled boxes correspond to F_{1y} and F_{2y} , respectively.

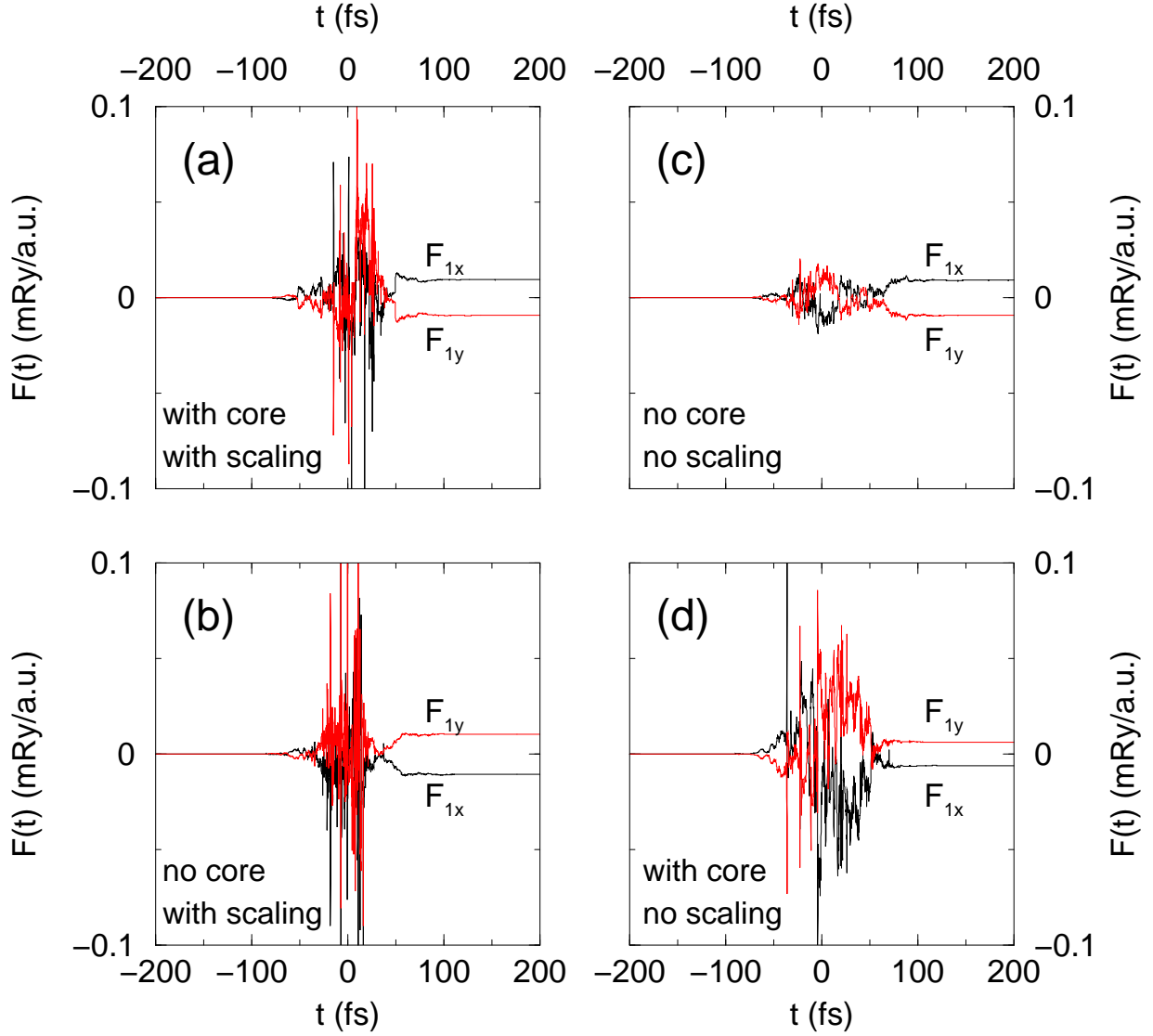


FIG. 3: Forces on atoms under four different conditions. (a) Energy window is between $[5,100]$, where the core states are included and the spin-polarization rescaling is used. (b) Energy window is between $[17,120]$ and does not include the core states. The spin rescaling is used. (c) Energy window is between $[17,120]$, where the core states are not included and the spin-polarization rescaling is not used. (d) Energy window is between $[5,120]$, where the core states are included and the spin-polarization rescaling is not used.

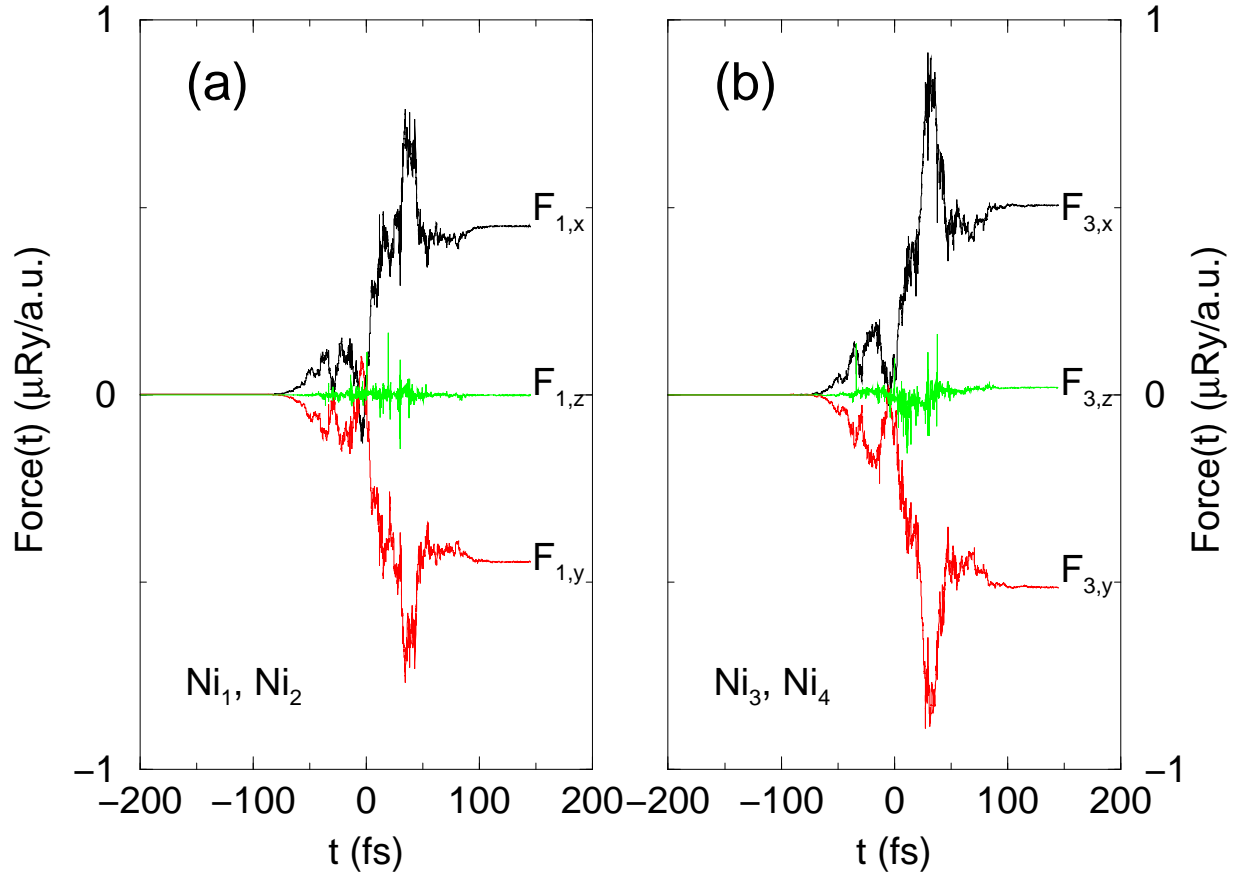


FIG. 4: Forces in bulk fcc Ni calculated with a simple cubic cell and four atoms in total. (a) Forces on Ni_1 . The force on Ni_2 is similar and not shown. To demonstrate the accuracy of our method, we remove all the symmetry operations, except the identity matrix. The k mesh is $14 \times 14 \times 14$. $R_{\text{MT}}K_{\text{max}}$ is 7. $\tau = 60$ fs. $A_0 = 0.015$ Vfs/ \AA . $\hbar\omega = 1.6$ eV. We use the circularly polarized light σ_{xy} . (b) Forces on Ni_3 . The force on Ni_4 is similar and not shown.